JBC Papers in Press. Published on December 28, 2007 as Manuscript M705884200
The latest version is at http://www.jbc.org/cgi/doi/10.1074/jbc.M705884200

Arginine biosynthesis in *Escherichia coli*: experimental perturbation and mathematical modeling

Marina Caldara[1,#], Geneviève Dupont[2,#], Frédéric Leroy[3], Albert Goldbeter[2], Luc De Vuyst[3] and Raymond Cunin[1,*]

Laboratory of Microbiology and Genetics[1], Vrije Universiteit Brussel, Pleinlaan 2, B-1050 Brussels, Belgium. Unité de Chronobiologie Théorique[2], Faculté des Sciences, Université Libre de Bruxelles, Campus Plaine, B-1050, Brussels, Belgium. Laboratory of Industrial Microbiology and Food Biotechnology[3], Vrije Universiteit Brussel, Pleinlaan 2, B-1050 Brussels, Belgium.

Running title: Modeling arginine biosynthesis in *E. coli*

# These authors contributed equally to this work

*Corresponding author
Mailing address: Laboratorium voor Erfelijkheidsleer en Microbiologie, Vrije Universiteit Brussel, Pleinlaan 2, 1050 Brussels, Belgium;Phone: 32-2-6291341 ;Fax: 32-2-6291473 ; e-mail: rcunin@vub.ac.be

Abstract

A basic challenge in cell biology is to understand how interconnected metabolic pathways are regulated to provide the adequate cellular outcome when changing levels of metabolites and enzyme expression. In *Escherichia coli*, the arginine and pyrimidine biosynthetic pathways are connected through a common metabolite provided by a single enzyme. The different elements of the arginine biosynthetic system of *Escherichia coli*, including the connection with pyrimidine biosynthesis, and the principal regulatory mechanisms operating at genetic and enzymatic levels were integrated in a mathematical model using a molecular kinetic approach combined with a modular description of the system. The model was then used to simulate a set of perturbed conditions: genetic derepression, feedback resistance of the first enzymatic step, low constitutive synthesis of the intermediate carbamyl phosphate. In all cases, an excellent quantitative agreement between simulations and experimental results was found. The model allowed to gain further insight into the function of the system, including the synergy between the different regulations. The outcome of combinations of perturbations on cellular arginine concentration was predicted accurately, establishing the model as a powerful tool for the design of arginine overproducing strains.

Introduction

One of the major aims of systems biology is to achieve a global understanding of metabolism by developing models able to describe and predict molecular and cellular functions at the level of whole metabolic pathways (1). Ultimately, the objective is to obtain comprehensive computer models of an entire living cell and all its functions. To attain such a goal, the International *Escherichia coli* Alliance (www.ecolicommunity.org) was launched in 2002 to consolidate global *E. coli* modeling efforts. As a part of this global project, we develop here a reliable mathematical model for arginine biosynthesis, based on the existing detailed knowledge of the principal regulatory mechanisms operating at both the genetic and the enzymatic levels of arginine metabolism (for reviews, see (2,3)) as well as on new experimental determinations. A molecular kinetic model will be used which is appropriate for the description of highly regulated systems, in particular to establish a hierarchy of the different regulatory mechanisms at work in the system (4). This model can then be used to predict arginine production in strains containing different modifications of the regulatory circuits.

Arginine constitutes about 5 % of the total proteins of *E. coli*. Arginine and its precursor ornithine are used for the biosynthesis of the most common polyamines, putrescine and spermidine, which are required for optimal growth through their involvement in several

physiological processes (3). In addition, under conditions of nitrogen starvation, arginine can be used as a (poor) nitrogen source by the arginine succinyltransferase pathway (5,6).

Arginine is synthesized from glutamate in eight enzymatic steps (FIG. 1). Five steps involving N-acetylated intermediates lead to ornithine, and three additional steps are required to convert ornithine into arginine (2,3). The biosynthetic enzymes are listed in Table I. The synthesis of all enzymes is subject to repression by arginine, mediated by the repressor ArgR. In addition, the first enzyme of the pathway, N-acetylglutamate synthase (NAGSase) is subject to feedback inhibition by arginine (7,8). In *E. coli*, a single carbamyl phosphate synthase (CPSase) provides carbamyl phosphate (CP) for both the arginine and the *de novo* pyrimidine biosyntheses (FIG. 1). Reflecting the dual function of CPSase, its synthesis is subject to cumulative repression by arginine and pyrimidines (9,10). In addition, CPSase activity is subject to a complex network of metabolic regulations: inhibition by UMP, antagonized by ornithine and IMP which are activators (11,12). CP is used for arginine biosynthesis by ornithine transcarbamylase (OTCase), an enzyme whose activity is not metabolically regulated. CP is also used by aspartate transcarbamylase (ATCase) in the first committed step of pyrimidine biosynthesis. The synthesis of ATCase is repressed by pyrimidines and its activity is synergistically inhibited by CTP and UTP, and activated by ATP (13,14).

Given the complex regulations of CPSase and ATCase, which enable the cell to respond to the challenge of providing CP for two pathways with sometimes conflicting demands, the balance of CP utilization between arginine and pyrimidine biosyntheses in different growth conditions cannot be predicted solely by an intuitive approach. The model presented here will be the first to describe in mathematical terms the distribution of the shared metabolite CP between the two biosynthetic pathways. More globally, in order to understand and describe arginine biosynthesis in quantitative terms, a simple mathematical model that can account for the experimentally observed steady-state levels of the various metabolites of the system needed to be developed. This model should also have the capability to describe the evolution of the concentrations of these metabolites during transitions between steady-states. In this study, we focus on a detailed and quantitative description of the arginine metabolic pathway; the evolution of the pyrimidine concentrations – whose levels affect the activities of both CPSase and ATCase – is described by phenomenological equations. A detailed modeling of pyrimidine biosynthesis in *E. coli* can be found elsewhere (15).

The naturally modular organization of complex metabolic systems can be exploited to simplify their quantitative description (16,17). In the model presented here, a simplification was introduced by representing the system as three modules, connected through a tightly regulated branch point. Each module comprises one key regulated step, the other steps within the module being considered as non-limiting for arginine biosynthesis and non-involved in other biological processes (FIG. 2). This simplified representation is supported by the results of a recent transcriptome analysis of the arginine regulon, which provided an integrated view of arginine regulation (18).

Parameter values from the literature and/or values determined experimentally for wild-type *E. coli* grown in the absence or in the presence of arginine will be used to develop the model. The model will then be used to determine corresponding steady-states in a set of perturbed conditions: a genetically derepressed strain (an *argR* mutant lacking an active repressor), a strain desensitized for feedback inhibition by arginine of the first biosynthetic step (a feedback-resistant NAGSase mutant), and a strain where a low constitutive synthesis of CP was engineered. Values obtained for all three simulated steady-states will be confronted with experimental measurements to validate the model. Finally, the model will be applied to get further insight into the function of the system, for instance by investigating the synergy between the various regulatory loops.

Experimental procedures

Chemicals

Chemicals are listed in the supplementary file *Experimental procedures*.

Strains and plasmids

P4X (Hfr, *metB*) is the wild-type strain for this study. P4X, a derivative of *E. coli* K-12 MG1655 through 58-161 and W6 (19), is the

strain in which previous studies on the arginine biosynthetic system were performed in the Laboratory of Microbiology and Genetics of the Vrije Universiteit Brussel.

P4XB2 (Hfr, *metB*, *argR*) is a genetically derepressed derivative of P4X.

P4XJEF8 (Hfr, *metB*, *thrA*, *ΔcarB-8*) harbours a deletion of part of *carB* (CPSase) which results in a double arginine/pyrimidine auxotrophy (20).

Primers used for construction of the following strains are listed in Table I in the supplementary file *Experimental procedures*.

P4XJEF8/pMAC2 (this study) contains plasmid pMAC2 carrying the *carAB* genes, complementing the *ΔcarB-8* defect. To construct the pMAC2 plasmid, the *carAB* genes were amplified by PCR from *E. coli* genomic DNA as a *Bgl*II-*Hind*III fragment (primers MC1; MC2). The fragment was then inserted into the suitably restricted pBAD/HisC plasmid (Invitrogen), under the control of the p_{BAD} promoter, to obtain pMAC2. pMAC2 was transformed into P4XJEF8, selecting for resistance to ampicillin. In the presence of glucose, *carAB* expression from p_{BAD} is strongly repressed (catabolite repression).

P4X/pKK*carAB* (21) contains a plasmid derived from pKK223-3 (Amersham Pharmacia; Buckinghamshire, UK) carrying wild-type *carAB* under the control of its own operator region.

P4XA1 (Hfr, *metB*, *argA-216*) (this study) contains the *argA-216* mutation conferring feedback resistance to NAGSase (22). To obtain this strain, a pBluescript®II (Stratagene, La Jolla, CA, USA) derivative p*argA-Kan* was first constructed, carrying the wild-type *argA* gene inserted as a *BamH*I-*Eco*RI PCR fragment (primers MC3; MC4) and a *Kan*^{r} cassette inserted as an *Eco*RI-*HindIII* PCR fragment (primers MC5; MC6).

The *argA216* point mutation (22) was then introduced by PCR amplification of the whole p*argA-Kan* plasmid using a set of complementary primers carrying the mutation (primers MC7; MC8) to obtain the p*argA216-Kan* plasmid. The *argA216* mutation was then introduced in the chromosome of the P4X strain using a recombineering method (23).

P4XA1-ΔR (this study) is a genetically derepressed derivative of P4XA1 in which *argR* was knocked-out using a recombineering method. A kanamycin resistance cassette was generated by PCR using primers with 50-nucleotides extensions homologous to sequences upstream and downstream of the *argR* coding sequence, then introduced in a P4XA1 strain expressing the λRed recombinase. Selecting for kanamycin resistance resulted in the recombinational replacement of the chromosomal *argR* region by the cassette. After selection, the resistance cassette was removed as described in Datsenko and Wanner (23).

P4XEC-1 (Hfr, *metB, ΔargEC-1*) (24) and PA342 (F$^-$, *ppc, argH-2, thr, leu, his, thi, str*^{r}) (25) were used in cross-feeding tests as indicators for the secretion of ornithine and arginine, respectively.

Cross-feeding experiments

Potential secretor and indicator strains were streaked side-by-side on minimal medium plates (26) containing the appropriate supplement and incubated at 37°C for the period of time required for cross-feeding in a positive control experiment. In the test for arginine secretion (indicator PA342), the supplement was: glucose (0.5 %, w/v), L-methionine (100 μg ml^{-1}), L-threonine (100 μg ml^{-1}), succinate (0.4 %, w/v), L-leucine (100 μg ml^{-1}), L-histidine (100 μg ml^{-1}) and thiamine (1 μg ml^{-1}). In the test for ornithine secretion (indicator P4XEC-1), the supplement was: glucose (0.5 %, w/v), L-methionine (100 μg ml^{-1}) and L-threonine (100 μg ml^{-1}).

Growth conditions

Cells were grown in flasks in a rotary shaker at 37°C in minimal medium (26) supplemented with 0.5 % (w/v) glucose and 0.67 mM L-methionine (100 μg ml^{-1}). When needed, 0.84 mM L-threonine (100 μg ml^{-1}) and 50 μg ml^{-1}ampicillin were added to minimal medium. Arginine-rich medium contained 0.47 mM L-arginine (100 μg ml^{-1}).

Cells were harvested at mid-log phase (OD_{660} = 0.5).

Determination of enzyme specific activities

Cellular extracts preparation and assays of NAGSase, OTCase and CPSase activities were performed as described in Caldara *et al*. (18).

ATCase activity was measured in the presence of 20 mM aspartate and 5 mM CP in 50 mM Tris-HCl buffer at pH 8. The carbamylaspartate formed was measured by

the colorimetric method of Prescott and Jones (27).
It should be stressed that activities were measured on dialyzed extracts so that they are true reflections of the amount of each protein present. The enzymatic activity values integrate genetic regulation and whatever posttranscriptional regulation operating on gene expression. (www.projectcybercell.com,(28)). Experiments were repeated at least five times for each condition of the system. Standard deviation was always lower than 20%.
Protein concentration was determined by the method of Lowry (29).

Metabolite extraction procedure

Cells were sampled, extracted and quenched following a protocol communicated by Dr. M.E. Wales (Dept of Biochemistry and Biophysics, Texas A&M University) with modifications. Cells in mid-log phase (OD_{660} = 0.5) were rapidly filtered in a Millipore vacuum manifold through 0.45 µm pore size MF™ membrane filters (Millipore). The filter was placed in a microcentrifuge tube containing 500 µl of 6 % TCA. The mixture was homogenized and placed on ice for 30 min. The metabolites were extracted adding an equal volume of freshly prepared 0.7 M tri-N-octylamine in 1,1,2-trichloro-1,2,2-trifluoroethane. After homogenization, the solution was incubated on ice for a further 30 min after which the aqueous phase was transferred to a clean tube.

Determination of intracellular free nucleotide concentrations

The analysis was carried out with a Waters High-Performance Liquid Chromatography system (Waters Corporation, Milford, MA, USA). Samples were injected using a Whatman Partisil 10 SAX column (250 x 4.6; 10 µm particle size), previously equilibrated with 1 mM ammonium phosphate pH 3.3 (buffer A). The nucleotides were eluted with a discontinuous gradient of buffer A and 750 mM ammonium phosphate pH 3.8 (buffer B), at a variable flow rate. Every run took 60 min to be completed. During the first 15 min the flow rate was 1.3 ml min^{-1} and only buffer A was present. In the next 25 min buffer B increased linearly to 100% at a flow rate of 1.5 ml min^{-1}. During the last 20 min, the column was brought back to the initial conditions (buffer A 100%, flow 1.3 ml min^{-1}). The peaks, detected by measuring the absorbance at 260 nm (UV detector, Waters Corp.) were identified with the help of appropriate external standards and the concentrations determined through integration with the Empower-Pro software (Waters Corp.).

Determination of intracellular free amino acid concentrations

For this analysis, the amino acids extracted were first derivatized using a ACCQ-kit (ACCQ: 6-aminoquinolyl-N-hydroxysuccininimidyl carbamate) purchased from Waters (Waters Corp.), 2-aminobutyric acid was added to each sample as an internal standard (IS). Amino acid concentrations were determined using a 2695 HPLC system (Waters Corp.) coupled to a Quattro Micro ™ mass spectrometer (Waters Corp.). The capillary column (symmetry C_{18}, 3.9 x 150 mm; 5 µm particle size, Waters Corp.) was kept at 35°C. The separation of the derivatized amino acids was carried out using a variable mobile phase with the solutions of 1 % formic acid in ultra-pure water (A) and 1 % formic acid in methanol (B). The gradient was as follows: 0 min: 90 % eluent A – 10 % eluent B, flow 0.15 ml min^{-1}; 45 min: 50 % eluent A – 50 % eluent B, flow 0.15 ml min^{-1}; 46 min: 20 % eluent A – 80 % eluent B, flow 0.15 ml min^{-1}; 80 min: 20 % eluent A – 80 % eluent B, flow 0.25 ml min^{-1}; 81 min: 90 % eluent A – 10 % eluent B, flow 0.25 ml min^{-1}; 90 min: 90 % eluent A – 10 % eluent B, flow 0.15 ml min^{-1}.The data were processed using the Masslynx 3.5 software (Waters Corp.).

Calculation of cellular maximal velocities

The model requires cellular maximal velocity (V_M) values for the different enzymatic activities considered: the maximal number of moles of substrate(s) that can be transformed in product(s) per unit of cellular volume and per unit of time. These are different from the V_{max} values for the enzymes, which are invariant, and they are calculated from the measured enzyme specific activities in each analyzed condition. The calculation method is described in the supplementary file *Experimental procedures*. Cellular maximal velocities will be represented as V_{MX} in the equations, where X is the initial of the enzyme considered.

Model development

The system was represented as three modules connected by a tightly regulated branch point (FIG. 2). The first module is the synthesis of ornithine from glutamate with NAGSase as key enzymatic activity; the second one is the synthesis of arginine from ornithine and CP with OTCase as key enzyme; the third module is the utilization of CP for *de novo* pyrimidine biosynthesis to produce ultimately UTP and CTP, with ATCase as key enzyme. The rigid branch point consists of CP synthesis from glutamine, bicarbonate, and ATP by CPSase, and the complex network of genetic and metabolic regulations controlling CP distribution between the arginine and the pyrimidine biosyntheses.

Evolution equations

The system represented in FIG. 2 is described mathematically by a set of five ordinary differential equations. The first one describes the evolution of ornithine concentration, represented by β. Knowing that the four steps between N-acetylglutamate, the product of the NAGSase reaction, and ornithine (β) are enzymatically non-regulated and assuming that they are fast, one can write

$$\frac{d\beta}{dt} = V_{NAGS} - V_{OTC} - V_{MF}\frac{\beta}{K_F + \beta} \quad \textbf{(1)}$$

where V_{NAGS} and V_{OTC} stand for the rates of the NAGSase and OTCase reactions, representing respectively the production and utilization of ornithine. The last term represents phenomenologically the consumption of ornithine for polyamine biosynthesis and ornithine secretion.

OTCase utilizes both ornithine (β) and CP (α) as substrates. CP, shared with the *de novo* pathway for pyrimidine biosynthesis, is produced by CPSase. Thus, its evolution in time is given by

$$\frac{d\alpha}{dt} = V_{CPS} - V_{OTC} - V_{ATC} \quad \textbf{(2)}$$

where V_{ATC} stands for the rate of the ATCase reaction, the first committed step of *de novo* pyrimidine biosynthesis.

The product of the OTCase reaction is citrulline. This intermediate is not explicitly considered in the model, as it is rapidly transformed into arginine (θ).

Arginine evolution is described by

$$\frac{d\theta}{dt} = V_{OTC} + P_a\theta_{ext} - V_{MU}\frac{\theta}{K_U + \theta} - k_S\theta \quad \textbf{(3)}$$

where $P_a\theta_{ext}$ stands for the rate of arginine uptake through the plasma membrane. This term has to be considered when the cells are grown in an arginine-rich medium. Arginine is used by *E. coli* for protein and polyamine synthesis, a process represented phenomenologically by a Michaelis-Menten term. Finally, in some conditions described further, arginine is secreted in the external medium; in such cases, the parameter k_S takes a value different from zero.

The ATCase reaction produces carbamylaspartate which is transformed to UMP (γ) in four subsequent enzymatic steps that are considered as non-limiting. UMP is in turn transformed in a few steps into CTP and UTP (δ). Pyrimidine biosynthesis is in itself a complex metabolic pathway (see ref. 15 for a detailed modeling study of pyrimidine biosynthesis in *E. coli*). Here, we describe the evolution of UMP, UTP and CTP in a phenomenological, simplified manner that simply allows us to reproduce the appropriate steady states for the pyrimidine concentrations. Those concentrations will thus provide the adequate feedback on arginine biosynthesis, which is the object of this study. The time evolution of UMP concentration (γ) is thus given by :

$$\frac{d\gamma}{dt} = V_{ATC} - k_2\gamma + J_O\frac{\gamma}{K_{pyr} + \gamma} \quad \textbf{(4)}$$

Parameter k_2 is the kinetic constant characterizing the transformation of UMP into CTP and UTP. The last term represents a complex set of pyrimidine nucleotide recycling and interconversion reactions, known as the salvage and interconversion pathways, respectively (31). J_0 stands for the maximal rate of UMP production by these pathways.This recycling process can function only if some UMP is provided by *de novo* synthesis, hence the second factor in this term, with K_{pyr} the concentration of UMP leading to a half-maximal effect.

As CTP and UTP could not always be measured separately, and as they act together on ATCase, they are lumped together as one variable (δ) in the model. The evolution of this

variable is simply represented by the input from UMP and a linear rate of use by the cell (k_3):

$$\frac{d\delta}{dt} = k_2\gamma - k_3\delta \qquad \textbf{(5)}$$

Enzymic rate equations

The next step is to give an appropriate expression for the rates of the four key enzymes (NAGSase, CPSase, ATCase and OTCase). NAGSase uses glutamate (S_1) and acetyl CoA (S_2) as substrates, and is feedback-inhibited by arginine (θ). To adequately model the experimental results of our study of NAGSase inhibition by arginine (32), the following kinetic expression is used:

$$V_{NAGS} = V_{MN}\frac{1}{1+\frac{\theta}{\rho(K_{i\theta}+\theta)}}\frac{S_1}{K_1+S_1}\frac{S_2}{K_2+S_2} \qquad \textbf{(6)}$$

where V_{MN} is the cellular maximal velocity of NAGSase, and K_1 and K_2 stand for the half-saturation constants of this enzyme by glutamate and acetyl CoA, respectively. $K_{i\theta}$ is the constant of inhibition by arginine and ρ is an adimensional factor that scales the effect of this inhibition. Rate expression **(6)** describes a partial, non-competitive inhibition of an enzyme (33).

CPSase has three substrates: bicarbonate (S_3), ATP (S_4), and glutamine (S_5). Ornithine (β) acts as a non-essential activator and UMP (γ) as a competitive inhibitor. Both effectors affect ATP binding. The rate expression for an enzyme regulated in this manner is given by (33):

$$V_{CPS} = V_{MC}\frac{S_3}{K_3+S_3}\frac{S_5}{K_5+S_5}\frac{\left(\frac{S_4}{K_4}+\frac{S_4\gamma}{\eta K_4 K_{I\gamma}}+\frac{S_4\beta}{\zeta K_4 K_{A\beta}}\right)}{\left(1+\frac{S_4}{K_4}+\frac{\gamma}{K_{I\gamma}}+\frac{\beta}{K_{A\beta}}+\frac{S_4\gamma}{\eta K_4 K_{I\gamma}}+\frac{S_4\beta}{\zeta K_4 K_{A\beta}}\right)} \qquad \textbf{(7)}$$

where K_3, K_4, and K_5 are the half-saturation constants for bicarbonate, ATP, and glutamine binding, respectively. V_{MC} stands for the cellular maximal velocity of CPSase. η scales the effect of UMP (γ) and ζ the effect of ornithine (β), while $K_{I\gamma}$ and $K_{A\beta}$ represent the concentrations of UMP and ornithine leading to half-maximal effects.

ATCase is a well studied allosteric enzyme (for a review, see (34)). A proper modeling of such an enzyme using, for instance, the Monod, Wyman, Changeux formalism (35) requires the knowledge of a very large set of parameter values. Here, a phenomenological expression that quantitatively reproduces experimental data was chosen (36). Because of the rapid turnover and highly efficient production of ATP, its intracellular free concentration was considered as being constant and saturating for the activation of ATCase ($K_{d\ app}$ = 1 mM), and K_6 in eqn. **(9)** is the apparent half-saturation constant for ATP-activated ATCase. A simple competitive inhibition by the CTP + UTP combination (δ) on aspartate (S_6) binding is considered. With CP (α) as the other substrate of ATCase, the rate equation is:

$$V_{ATC} = V_{MA}\frac{\alpha}{K_{\alpha 2}+\alpha}\frac{S_6^{n6}}{K_6^{'n6}+S_6^{n6}} \qquad \textbf{(8)}$$

where V_{MA} is the cellular maximal velocity of ATCase, $K_{\alpha 2}$ the half-saturation constant for carbamyl phosphate (α), K_6 the apparent half-saturation constant for aspartate (S_6) in the presence of ATP, and n_6 the Hill coefficient for the saturation by this compound. The inhibitory effect of CTP and UTP (δ) is taken into account by using:

$$K_6^{'} = K_6\left(1+\left(\frac{\delta}{K_{i\delta}}\right)\right) \qquad \textbf{(9)}$$

where $K_{i\delta}$ is the inhibition constant for δ (CTP + UTP).

OTCase catalyses the transformation of ornithine (β) and carbamyl phosphate (α) into citrulline that finally leads to arginine through two rapid, non-regulated steps. OTCase itself is not regulated, and thus :

$$V_{OTC} = V_{MO}\frac{\alpha}{K_{\alpha 1}+\alpha}\frac{\beta}{K_\beta+\beta} \qquad \textbf{(10)}$$

where V_{MO} is the cellular maximal velocity of OTCase, $K_{\alpha 1}$ the half-saturation constant for carbamyl phosphate (α), and K_β the half-saturation constant for ornithine (β).

The set of eqs. **(1)-(10)** defines the kinetic model for arginine biosynthesis. These equations were integrated using the XPPAUT software (37) choosing a numerical method appropriate for "stiff" differential equations.

Parameter values

As a system, arginine biosynthesis is defined by a large number of parameters. Forty-eight of these are incorporated in the model. For thirty-six of these, values were determined experimentally in this study or obtained from the literature. For the remaining twelve parameters, for which experimental determination methods are currently not sensitive enough, values were estimated manually to obtain the appropriate steady-states for the wild-type in minimal and arginine-rich media. Thus the estimated parameter values of Tables II and IIIA were obtained by manual adjustment, without using any minimization criterion. The fit was considered satisfactory when the difference between the steady-states obtained by simulation and experimentally did not exceed the experimental error. Several parameters are characteristic of components of the system and will not vary in the present analysis. This is the case for half-saturation constants, and adimensional factors characterizing enzyme activities. A list of the values for the parameters that do not change with strains or experimental conditions is given in Table II. Values for the other parameters, including substrate concentrations and enzymatic cellular maximal velocities, were determined experimentally in all conditions tested. These values are presented in Table IIIA for the model calibration and in Table IV for the other conditions tested.

For simplicity, substrate concentrations (S_1 to S_6) are considered as parameters and not as variables. Although these substrates are consumed in the course of time, it is assumed that they are rapidly replenished or that their specific consumption in the arginine/pyrimidine biosynthesis is negligible compared to their consumption in other cellular processes such as, for instance, protein synthesis. This is indeed supported, for amino acid substrates and ATP, by comparisons of the global biosynthetic requirements for these metabolites with the chemical composition of *E. coli* (38), and with the free concentrations measured in this study. For instance, the specific arginine cellular content corresponds to less than 4 % of the total amount of glutamate that must be synthesized by the cell. Also, in the growth conditions used, the cell secretes acetate derived from accumulating acetyl CoA (39), which is thus present in non-limiting amounts for arginine synthesis.

In addition, regarding these assumptions, a test was run by introducing evolution equations for the substrates. From a modeling point of view, the introduction of evolution equations for substrates S1 to S6 taking into account their major implication in other cellular processes leads to only minor changes in the steady state concentrations for the metabolites involved in arginine biosynthesis (the results are presented in the supplementary file *Extension of the model to consider the evolution of substrate concentrations*).

Variable values

The variables of the system are intracellular metabolite concentrations. Values for the variables determined experimentally and computed by means of the model are compared in Table IIIB (calibration) and Table V (validation).

Results

Model calibration

Two metabolic steady-states of arginine biosynthesis in wild-type *E.* coli were used to calibrate the model: partial repression due to endogenous free arginine (growth in minimal medium) and full repression, where the intracellular arginine concentration is augmented by the uptake of arginine from the medium (arginine-rich medium). Experimentally determined values for the parameters are shown in Table IIIA. The values for the variables of the system, observed experimentally and computed by means of the model are compared in Table IIIB.

The values obtained with the model are in excellent agreement with the experimental determinations, well within the experimental error. No sufficiently sensitive and accurate method is currently available to measure CP, which is present at very low concentration in most conditions tested (excepting full repression) and is also extremely unstable. Ornithine concentration was always around or below the level of accurate determination. Note that when this intermediate accumulates (see further) it can be measured accurately.

A 10-fold increase of the free arginine concentration is observed in cells grown in arginine-rich medium. This is due to the uptake of arginine from the medium, which masks the

effects of repression and feedback inhibition on endogenous arginine synthesis. An estimate of the arginine concentration synthesized in conditions of repression was obtained by measuring intracellular arginine in cells grown in the presence of decreasing amounts of extracellular arginine in the medium. The steady-state level of intracellular arginine first decreases linearly, then increases again up to 0.14 mM when extracellular arginine concentration becomes zero (data not shown) because the effects of repression and feedback-inhibition diminish in this condition. If the linear decreasing part of the curve is extrapolated to zero extracellular arginine, a theoretical value of 0.012 mM for the steady-state intracellular concentration is obtained, which corresponds to a "virtual" condition in which repression and feedback-inhibition would still exert their full effect without arginine being present in the medium, and a factor of 12 can be deduced for their combined effects. This is close to the factor 10 calculated by combining the measured 2-fold repression of NAGSase cellular activity (Table IIIA, V_{MN} in arginine-rich medium compared to minimal medium) and the 5-fold feedback inhibition of its activity in the presence of arginine (32).

The model predicts an accumulation of CP in conditions of full arginine repression. However, as explained above, no sensitive and accurate method is currently available to verify this experimentally. This accumulation would signify that ornithine concentration has become limiting for CP utilization in arginine biosynthesis but also that little CP is used for pyrimidine biosynthesis in these conditions. The pyrimidine nucleotide pools, however, are similar in the presence and in the absence of arginine (Table IIIB). Alternatively, CP accumulation could be a consequence of the low free aspartate concentration (S_6 = 0.30 mM), much below the apparent half-saturation concentration of ATCase by this substrate (K_6 = 7 mM). Adding aspartate (5 mM) to the growth medium to boost the ATCase reaction did not increase the nucleotide pools (Table IIIB, lines marked with an asterisk), although the intracellular free aspartate concentration was then 2 mM. The predicted CP accumulation and the apparently low consumption for pyrimidine synthesis must then be ascribed to a tight regulation of the flux through the *de novo* pathway rather than to a limiting free aspartate concentration.

A sensitivity analysis of the model was performed by varying the values of all the parameters by +20 % and -20 %. While relatively large variations of the steady-state concentrations of intermediate metabolites were obtained, the concentrations of the end-products were only weakly affected, showing the robustness of the model (these data are presented in the supplementary file *Sensitivity analysis*).

Model validation

Steady-states were simulated for three perturbed conditions of the system, each corresponding to the abolition of one regulatory mechanism. Two of these perturbed states result from a single mutational event, the third one involves a more complex genetic modification. Genetic regulation is not incorporated explicitly in the model but it is accounted for by its effect on enzyme concentrations, which were again measured for each perturbed condition. These changed enzyme concentrations are incorporated in the model as different values for the cellular maximal velocities (see Material and Methods). These values are shown in Table IV, together with the values of the other parameters associated with these mutants. The value of K_4 was adapted to take into account its dependence on the IMP concentration (21). J_o, k_2, and k_3 (all associated with pyrimidines) are fitted to get the appropriate steady-state values for δ and γ. Parameter k_s is also adapted to take into account the up-regulation of arginine secretion in case of high intracellular arginine concentrations (40). Anyway, these parameters classified as 'estimated' in Table IV play a minor role as compared to enzymatic processes, which is reflected in the sensitivity analysis by the fact that a change of + or – 20% of the value of J_0, k_2, k_3 or k_s induces a change of maximum 8% in the steady state level for arginine (see supplementary file *Sensitivity analysis*).The steady-states predicted by the model are compared with experimental observations in Table V.

Genetic derepression: an argR mutant.

The arginine-bound ArgR repressor blocks the initiation of transcription of the arginine biosynthetic genes by binding to operator loci overlapping the different promotor regions. The synthesis of the repressor itself is partially autoregulated (41,42). In an *argR* mutant, the

repressor is inactive. Genetic derepression increases the concentrations (and specific activities) of NAGSase, CPSase, and OTCase (FIG. 1). The values of V_{MN}, V_{MC}, and V_{MO} increase accordingly in the model. The arginine uptake term ($P_a\theta_{ext}$) also increases, because the uptake systems are also derepressed in this mutant (18).

In minimal medium, a 5- to 6-fold increase of the arginine concentration compared to wild-type was observed (0.83 mM instead of 0.14 mM, Table V). The model would predict a higher increase unless a significant value is attributed to arginine secretion out of the cell (k_s = 0.002 min^{-1} instead of 0 for the wild-type). The occurrence of secretion was verified by cross-feeding of an *argH* mutant by the *argR* strain on minimal medium (FIG. 3, A).

In arginine-rich medium, the arginine concentration increased even further than in the wild-type (3.40 mM compared to 1.55 mM, see Tables IIIB and V): this reflects the derepression of the two major arginine uptake systems, which are part of the arginine regulon (18).

Genetic derepression of arginine biosynthesis induces a new steady-state of the pyrimidine system: the pyrimidine nucleotide pools are two times higher in the *argR* mutant than in the wild-type, whereas the ATCase cellular activity is two times lower (Table IV). This could result from an altered CP distribution between the two systems but the underlying mechanism is not clear. In the model, this effect was phenomenologically described by changing J_o, the rate of UMP generation by the salvage and interconversion pathways, from 0.090 to 0.180 mM min^{-1} (Table IV).

Cancellation of feedback inhibition: a feedback-resistant mutant of NAGSase.

In the feedback-resistant mutant P4XA-1, the fbr-NAGSase has a 35-fold reduced affinity for arginine (Table II) but its V_{max} is the same as that of the native enzyme (32). The value of $K_{i\theta}$ is modified accordingly in eq. **(6).** The model predicts a 6-fold increase of arginine concentration when cells are grown in minimal medium, which is verified experimentally (Table V). The amplitude of this increase is similar to that observed in the *argR* mutant described above. Here too, the predicted secretion of arginine was verified by a cross-feeding test (FIG. 3, B). The predicted increase of arginine concentration due to uptake from the arginine-rich medium is also verified experimentally.

Limitation of CP synthesis: a strain with low constitutive CPSase expression

In this strain (P4XJEF8/pMAC2), the cumulative transcriptional repression of the CPSase genes (*carAB*) by arginine and pyrimidines is abolished. Instead, CPSase synthesis is controlled by carbon catabolite repression and is therefore low in cells grown with glucose as the sole carbon source. Indeed, the value for the cellular maximal velocity of CPSase is reduced significantly (V_{MC}, Table IV, third column). The residual CPSase activity is still subject to metabolic regulations in this mutant. A significant physiological derepression of OTCase is observed, less so for NAGSase (Table IV). ATCase is derepressed too (Table IV).

The model predicts a similar 0.10 mM reduction of arginine concentration in minimal and in arginine-rich medium. This is indeed verified experimentally (Table V). The predicted ornithine accumulation (0.38 mM) in minimal medium is also verified. At this concentration, secretion of ornithine is expected and it was detected by the cross-feeding of P4XEC-1 (*argEC-1*) but not of PA342 (*argH-2*) on minimal medium (FIG. 3, D and E).

CP limitation is associated with a change in the rate of the pyrimidine salvage pathways (J_o). To fit with the unchanged 1.52 mM (CTP+UTP) concentration, the phenomenological rate of (CTP+UTP) utilization was reduced (Table V). This can be justified by the slower growth of this strain (a doubling time of 90 min instead of 60 min for all the other strains in this study) and a concomitant reduced consumption of nucleotides for nucleic acid synthesis.

Applications

The model provides a good quantitative description of arginine biosynthesis in *E. coli*. It can therefore be applied to describe the variation of the pools of metabolic intermediates in response to simulated parameter changes and to predict arginine production in strains combining different modifications of the regulatory circuits.

Variation of arginine concentration as a function of CPSase activity

It was shown above that a striking decrease of arginine concentration is observed in a mutant where CP synthesis is limited (P4XJEF8/pMAC2 grown on glucose), suggesting that CP synthesis is rate-limiting for arginine biosynthesis (Table V). The effect of increasing V_{MC} on arginine concentration was investigated in greater detail. FIG. 4 shows the predicted variation of arginine, ornithine, and CP concentrations as CPSase cellular maximal velocity is increased from 0.2 to 2.5 mM min^{-1}. As CP concentration increases slightly, arginine concentration increases. As a result, ornithine concentration decreases under the combined effects of its utilization for arginine synthesis and of arginine repression. Above a V_{MC} of about 2.3 mM min^{-1} (about the V_{MC} value for the wild-type in minimal medium), CP stops being limiting for arginine synthesis. Instead, ornithine becomes the limiting metabolite. As a consequence, arginine concentration should not increase with further augmentation of V_{MC} (FIG. 4). This was verified experimentally using a wild-type strain containing extra copies of *carAB*, the operon coding for CPSase (strain P4X/pKK*carAB*), grown in minimal medium: arginine concentration stayed about 0.15 mM even when V_{MC} was 3.7 mM min^{-1}.

Combined alterations of regulatory circuits

The model was also applied to explore conditions in which arginine production could be maximized. Combinations of alterations of regulatory circuits were simulated, as well as a 2-fold increase of the concentration of the initial substrate glutamate (S_1 = 14 mM instead of 7 mM). According to the model, doubling the glutamate concentration should increase the arginine concentration almost 2-fold (FIG. 5, C). Indeed, with a K_m of 25 mM for glutamate, NAGSase functions well below its saturation by that substrate. Unexpectedly, doubling glutamate concentration and setting CPSase capacity (V_{MC}) at 2.5 mM min^{-1}, the value at which CP concentration stops being limiting (see FIG. 4), should not increase arginine concentration further (FIG. 5, D). In contrast, doubling the glutamate concentration in the feedback-resistant NAGSase mutant (P4XA1) should increase arginine concentration 2-fold (FIG. 5, G). Remarkably, a combination of the feedback-resistant *argA-216* and *argR* mutations should drastically increase the cellular arginine concentration: an 80-fold increase (11 mM), calculated after introducing a term for secretion (k_s = 0.002 min^{-1}). Thus the model predicts that abolishing both the genetic and the metabolic control of arginine on its own biosynthesis has an effect of an amplitude that exceeds by far the sum of the effects of each separate perturbation. This amplification most probably originates from the highly non-linear character of the various processes involved in the regulation of the pathway.

This prediction was tested experimentally by constructing a double *argA-216 argR* mutant (P4XA1-ΔR). In minimal medium, the measured fold change of arginine concentration is 85 (12 ± 0.5 mM) (FIG. 5, H). Resulting from the increased arginine production, increased secretion by that strain is also observed: cross-feeding by the double mutant allows the streak of an *argH* indicator strain to grow fully after 16 hours incubation at 37 °C on minimal medium (FIG. 3 C), whereas 50 hours are required to elicit an equivalent growth with arginine secreted by either the *argR* (P4XB2) or the *argA-216* (P4XA1) mutant (FIG. 3, A and B).

Discussion

To date, only a few amino acid biosyntheses in *E. coli* have been modeled successfully using a kinetic approach supported by experimental measurements: threonine (43) and branched chain amino acids (44). The molecular kinetic model for arginine biosynthesis in *E. coli* presented here takes into account the complex network of genetic and metabolic regulations at work in the system as well as its interaction with the *de novo* pyrimidine biosynthesis through the sharing of the common metabolite CP. Such a holistic approach is required to integrate and fully understand the extensive biological knowledge available about an analyzed system and to obtain novel insights into it (45,46)

Modular organization in biological systems has been extensively described (16,47,48) and its exploitation for modeling purposes was reported and found particularly effective when the final aim is to integrate the developed model in a more complex one (17,49-51). To describe arginine biosynthesis, four modules have been considered, each containing one key enzyme. All the key enzymatic reactions have been defined using classical kinetic rate

expressions. The resulting model predicts accurately arginine concentrations in different steady-states corresponding to perturbed conditions of the system. This quantitative accuracy results, in part, from the large number of parameters (forty-eight) incorporated in the model and from the fact that for thirty-six of these, values could be obtained from the literature or determined experimentally.

In some conditions associated with a high rate of arginine synthesis, the model must contain a term for arginine secretion to account for the experimentally determined steady-states. Secretion was reported previously for genetically derepressed strains (25). This was indeed observed in this study. In addition, the model predicts secretion of arginine by a feedback-resistant mutant of the first enzyme NAGSase. This was verified experimentally by the cross-feeding of an *argH* mutant.

The concentration of the arginine precursor ornithine was close to or below detection level (0.02 mM) in almost all conditions tested, but its predicted accumulation in a mutant with low CPSase activity was verified (Table V). In addition, the model predicts that ornithine should be secreted in this condition, which was shown by the cross-feeding of an *argEC* but not of an *argH* mutant.

Surprisingly, in a feedback-resistant mutant of NAGSase, the levels of the various enzymes associated with arginine biosynthesis remain nearly unchanged as compared to the wild-type, although the arginine concentration in this mutant on minimal medium is 6 times higher than in the wild-type (see Table IV). Further investigations (Caldara *et al*., in preparation) demonstrated that in the wild-type as in the mutant, a threshold intracellular arginine concentration of about 0.90 mM needs to be achieved to establish full repression. This phenomenon that cannot be explained solely by the partial autoregulation of repressor synthesis (18,41,42) is currently being investigated, which could lead to the discovery of an as yet unidentified regulatory loop (Caldara *et al*., in preparation).

A major interest of the model is that it provides a first quantitative description of the regulation of CPSase which has to balance the demands of arginine and pyrimidine biosyntheses. A simulated variation of CPSase concentration shows quite well how CP production is a regulator of the metabolic flux through the arginine pathway (FIG. 4): up to a CPSase synthetic capacity of 2.3 mM min^{-1}, CP concentration is limiting; above this threshold, ornithine concentration becomes the limiting factor. Remarkably, CPSase capacity in the wild-type *E. coli* in minimal medium is just below this threshold value at 2.10 mM min^{-1}, showing how the rigid branch point of the system is finely poised to respond to metabolic regulatory signals.

Several observations relevant to the cross-talk between the arginine and *de novo* pyrimidine pathways should be mentioned. Arginine itself never has a direct effect on pyrimidine nucleotides concentrations. Indeed, in none of the steady-states tested were the concentrations of pyrimidine nucleotides affected by the size of the free arginine pool, even when increased nucleotides concentrations are observed in an *argR* mutant (genetic derepression, Table V). In an *argR* mutant, a partial derepression of CP synthesis and an increased demand of CP for arginine synthesis occur simultaneously. If the resulting new balance between CP production and consumption shows a deficit, an effect on the *de novo* pyrimidine synthesis, possibly a derepression, could be expected. Instead, an increase of the pyrimidine nucleotide concentrations and a concomitant repression of ATCase capacity were observed (Tables IV and V), which could indicate a greater availability of CP for pyrimidine synthesis. However, when the model predicts an increased availability of CP, as in wild-type *E. coli* on arginine-rich medium, the pyrimidine nucleotides concentrations are unchanged compared to minimal medium conditions (Table IIIB). The relationship between CP availability and pyrimidine nucleotides pools is therefore not a simple one and the contribution of the pyrimidine salvage pathways must also be taken into consideration. Besides, the low concentration of free aspartate (S_6 in the 0.20 to 0.36 mM range) means that ATCase functions well below its cellular K_m (K_6) of 7 mM and therefore that *de novo* pyrimidine synthesis fulfils an anaplerotic function, the maintenance of pyrimidine nucleotide pools being mainly ensured by recycling through the salvage pathways. This stresses the importance of the inclusion in the model of a term (J_o) accounting for the salvage pathways contribution. Of course, pyrimidine synthesis is not modeled in detail here and J_o is just a phenomenological term representing other

sources of pyrimidines than the *de novo* biosynthesis. Inclusion of this term allows to reproduce accurately pyrimidine nucleotide concentrations. What came as a surprise was the importance of the contribution of the recycling pathway to the pyrimidine nucleotide pools, which could not have been expected on an intuitive basis.

Interestingly, an anaplerotic role for *de novo* synthesis is also assumed in a model specifically aimed at describing pyrimidine biosynthesis (15). In that study, it appears that most of the cellular UMP is provided by uracil phosphoribosyl transferase, thus by the salvage pathway, and that the amount of pyrimidines originating from CP transformation is comparatively small**.**

As far as arginine synthesis is concerned, our study shows that metabolic regulation of the first enzyme of the pathway and genetic repression have quantitatively similar contributions to the control of the metabolic flux through the pathway. Moreover, when either one of these regulations is abolished, only a modest increase (5 to 6 times) in arginine production can be obtained (FIG. 5, E and F), suggesting the presence of a backup mechanism as often observed in regulatory circuits (52). In contrast, in a double mutant of *E. coli* where both metabolic and genetic control of NAGSase activity by arginine are suppressed, the free arginine concentration increases 80 times (FIG. 5, H). As this surprising result was first predicted by the model, then verified experimentally, the model appears as a powerful tool to get a detailed understanding of this highly complex biosynthetic pathway as well as to design arginine overproducing strains.

Escherichia coli possesses a linear pathway for arginine biosynthesis. However, a large number of microorganisms present a so-called acetyl cycle pathway in which the acetyl group is transferred from acetylornithine to glutamate by an ornithine acetyltransferase (OATase). In that case, NAGSase fulfils an anaplerotic function and the second enzyme of the pathway - N-acetylglutamate kinase (NAGKase) - becomes the target for feedback-inhibition by arginine. In *Pseudomonas aeruginosa,* both NAGSase and NAGKase are inhibited by arginine (53), a situation reminiscent of that found in the yeast *Saccharomyces cerevisiae* and *Neurospora crassa* (54,55). This variety of pathway organizations and the discovery in *Xhantomonas campestris* of yet another type of pathway in which acetylcitrulline is formed from acetylornithine prior to deacetylation (56), has led to a recent reappraisal of the evolution of the pathway in microorganisms (57). The successful modeling approach presented here can be applied to describe these various pathways for arginine biosynthesis and, coupled with a sensitivity analysis, to evaluate their relative performance in terms of control.

In this study, the analysis of the model has been restricted to the prediction of the steady-state values of the metabolites. However, the integration of the evolution equations of the system can also lead to predictions about the dynamics of the pathway. Such numerical results should then have to be compared with dynamical observations of the concentrations of the various metabolites. The present model could also be extended to model the dynamics of genetic regulation. This approach would provide interesting comparative information about the time courses of metabolic and genetic control of arginine biosynthesis. In a much more speculative way, one could also use the model to find out experimental conditions that could possibly lead to sustained oscillations in arginine concentration (58). Such an oscillatory behavior has indeed been observed in many other highly non linear regulatory networks (59) combining positive and negative feedbacks.

Acknowledgements

The authors thank Gino Vrancken for performing LC-MS measurements. RC and LDV acknowledge support from the Research Council of the Vrije Universiteit Brussel (grant #OZR837) and the Fund for Scientific Research-Flanders (FWO-Vlaanderen, #G.0041.03). GD and AG acknowledge support from the Fonds de la Recherche Scientifique Médicale (grant #3.4636.04), the European Union through the Network of Excellence BioSim (Contract #LSHB-CT-2004-005137) and the Belgian Programme on Interuniversity Attraction Poles, initiated by the Belgian Federal Science Policy Office, project #P6/22 (BIOMAGNET). GD is Maître de Recherche at the Belgian Fonds National de

la Recherche Scientifique. FL is a postdoctoral fellow of the FWO-Vlaanderen.

References

1. Bruggeman, F. J., and Westerhoff, H. V. (2007) *Trends Microbiol* **15**, 45-50
2. Cunin, R., Glansdorff, N., Piérard, A., and Stalon, V. (1986) *Microbiol Rev* **50**, 314-352
3. Charlier, D., and Glansdorff, N. (2004) *Biosynthesis of arginine and polyamines.*, ASM Press, *In* A. Böck, R.Curtiss, J.B. Kaper, F.C. Neidhardt, T. Nyström, K.E. Rudd, and C.L. Squires (ed.), EcoSal-*Escherichia coli* and *Salmonella*: cellular and molecular biology. (on line) http://www.ecosal.org Washington D.C.
4. Goldbeter, A. (2002) *Nature* **420**, 238-245
5. Schneider, B. L., Kiupakis, A. K., and Reitzer, L. J. (1998) *J Bacteriol* **180**, 4278-4286
6. Lu, C. D. (2006) *Appl Microbiol Biotechnol* **70**, 261-272
7. Vyas, S., and Maas, W. K. (1963) *Arch Biochem Biophys* **100**, 542-546
8. Leisinger, T., and Haas, D. (1975) *J Biol Chem* **250**, 1690-1693
9. Piérard, A., Glansdorff, N., Mergeay, M., and Wiame, J. M. (1965) *J Mol Biol* **14**, 23-36
10. Piette, J., Nyunoya, H., Lusty, C. J., Cunin, R., Weyens, G., Crabeel, M., Charlier, D., Glansdorff, N., and Pierard, A. (1984) *Proc Natl Acad Sci U S A* **81**, 4134-4138
11. Anderson, P. M., and Meister, A. (1966) *Biochemistry* **5**, 3164-3169
12. Piérard, A. (1966) *Science* **154**, 1572-1573
13. Gerhart, J. C., and Pardee, A. B. (1962) *J Biol Chem* **237**, 891-896
14. Wild, J. R., Loughrey-Chen, S. J., and Corder, T. S. (1989) *Proc Natl Acad Sci U S A* **86**, 46-50
15. Rodriguez, M., Good, T. A., Wales, M. E., Hua, J. P., and Wild, J. R. (2005) *J Theor Biol* **234**, 299-310
16. Hartwell, L. H., Hopfield, J. J., Leibler, S., and Murray, A. W. (1999) *Nature* **402**, C47-52
17. Bruggeman, F. J., Westerhoff, H. V., Hoek, J. B., and Kholodenko, B. N. (2002) *J Theor Biol* **218**, 507-520
18. Caldara, M., Charlier, D., and Cunin, R. (2006) *Microbiology* **152**, 3343-3354
19. Bachmann, B. J. (1987) *Derivations and genotypes of some mutant derivatives of Escherichia coli K-12.*, 2nd Ed., ASM Press, Washington, D.C.
20. Mergeay, M., Gigot, D., Beckmann, J., Glansdorff, N., and Piérard, A. (1974) *Mol Gen Genet* **133**, 299-316
21. Delannay, S., Charlier, D., Tricot, C., Villeret, V., Piérard, A., and Stalon, V. (1999) *J Mol Biol* **286**, 1217-1228
22. Rajagopal, B. S., DePonte, J., 3rd, Tuchman, M., and Malamy, M. H. (1998) *Appl Environ Microbiol* **64**, 1805-1811
23. Datsenko, K. A., and Wanner, B. L. (2000) *Proc Natl Acad Sci U S A* **97**, 6640-6645
24. Elseviers, D., Cunin, R., and Glansdorff, N. (1972) *Mol Gen Genet* **117**, 349-366
25. Glansdorff, N., and Sand, G. (1965) *Biochim Biophys Acta* **108**, 308-311
26. Glansdorff, N. (1965) *Genetics* **51**, 167-179
27. Prescott, L. M., and Jones, M. E. (1969) *Anal Biochem* **32**, 408-419
28. Sundararaj, S., Guo, A., Habibi-Nazhad, B., Rouani, M., Stothard, P., Ellison, M., and Wishart, D. S. (2004) *Nucleic Acids Res* **32**, D293-295
29. Lowry, O. H., Rosbrough, N. J., Farr, A. L., and Randall, R. J. (1965) *J Biol Chem* **193**, 265
30. De Staercke, C., Van Vliet, F., Xi, X. G., Rani, C. S., Ladjimi, M., Jacobs, A., Triniolles, F., Hervé, G., and Cunin, R. (1995) *J Mol Biol* **246**, 132-143
31. Neuhard, J., and Kelln, R. A. (1996) *Biosynthesis and converisons of pyrimidines.*, II Ed., ASM Press, *In* A. Böck, R.Curtiss, J.B. Kaper, F.C. Neidhardt, T. Nyström, K.E. Rudd, and C.L. Squires (ed.), EcoSal-*Escherichia coli* and *Salmonella*:cellular and molecula biology.(on line)http://www.ecosal.org Washington D.C.

32. Caldara, M. (2007) *Ph.D. Thesis; Vrije Universiteit Brussel*
33. Segel, I. (1993) *Enzyme kinetics*, Wiley, New York
34. Hervé, G. (1989) *Aspartate transcarbamylase from Escherichia coli. In Allosteric enzymes*, CRC Press, Boca Raton FL
35. Monod, J., Wyman, J., and Changeux, J. P. (1965) *J Mol Biol* **12**, 88-118
36. Wales, M. E., and Wild, J. R. (1999) *Aspartate transcarbamoylase. In Creighton,TE.,Encyclopedia of molecular biology;* Wiley, New York
37. Ermentrout, B. (2002) *Simulating, analyzing, and animating dynamic systems: a guide to XPPAUT for researchers and students.*, 1st Ed., SIAM, New York
38. Reitzer, L. (2003) *Annu. Rev. Microbiol*. **57,**155-176
39. Kumari, S., Beatty, C.M., Browning, D.F., Busby, S.J.W., Simel, E.J., Hovel-Miner, G. and Wolfe, A.J. (2000) *J. Bacteriol.* **182**, 4173-4179
40. Nandinendi, M.R., and Gowrishankar, J. (2004) *J. Bacteriol.* **186,** 3539-3546
41. Lim, D. B., Oppenheim, J. D., Eckhardt, T., and Maas, W. K. (1987) *Proc Natl Acad Sci U S A* **84**, 6697-6701
42. Maas, W. K. (1994) *Microbiol Rev* **58**, 631-640
43. Chassagnole, C., Rais, B., Quentin, E., Fell, D. A., and Mazat, J. P. (2001) *Biochem J* **356**, 415-423
44. Yang, C. R., Shapiro, B. E., Hung, S. P., Mjolsness, E. D., and Hatfield, G. W. (2005) *J Biol Chem* **280**, 11224-11232
45. Kitano, H. (2002) *Science* **295**, 1662-1664
46. Stelling, J., and Gilles, E. D. (2004) *IEEE Trans Nanobioscience* **3**, 172-179
47. Lauffenburger, D. A. (2000) *Proc Natl Acad Sci U S A* **97**, 5031-5033
48. Ravasz, E., Somera, A. L., Mongru, D. A., Oltvai, Z. N., and Barabasi, A. L. (2002) *Science* **297**, 1551-1555
49. Bruggeman, F. J., and Kholodenko, B. N. (2002) *Mol Biol Rep* **29**, 57-61
50. Castellanos, M., Wilson, D. B., and Shuler, M. L. (2004) *Proc Natl Acad Sci U S A* **101**, 6681-6686
51. Qi, Y., and Ge, H. (2006) *PLoS Comput Biol* **2**, e174
52. Kafri, R., Bar-Even, A., and Pilpel, Y. (2005) *Nat Genet* **37**, 296-299
53. Haas, D., Kurer, V., and Leisinger, T. (1972) *Eur J Biochem* **31**, 290-295
54. Abadjieva, A., Pauwels, K., Hilven, P., and Crabeel, M. (2001) *J Biol Chem* **276**, 42869-42880
55. Yu, Y. G., Turner, G. E., and Weiss, R. L. (1996) *Mol Microbiol* **22**, 545-554
56. Shi, D., Morizono, H., Yu, X., Roth, L., Caldovic, L., Allewell, N. M., Malamy, M. H., and Tuchman, M. (2005) *J Biol Chem* **280**, 14366-14369
57. Xu, Y., Labedan, B., and Glansdorff, N. (2007) *Microbiol Mol Biol Rev* **71**, 36-47
58. Goldbeter, A. (1973) *PhD thesis.Université Libre de Bruxelles*
59. Hess, B., and Boiteux, A. (1971) *Annu Rev Biochem* **40**, 237-258
60. Marvil, D. K., and Leisinger, T. (1977) *J Biol Chem* **252**, 3295-3303
61. Anderson, P. M., and Meister, A. (1965) *Biochemistry* **4**, 2803-2809
62. Rubio, V., Cervera, J., Lusty, C. J., Bendala, E., and Britton, H. G. (1991) *Biochemistry* **30**, 1068-1075
63. Robin, J. P., Penverne, B., and Hervé, G. (1989) *Eur J Biochem* **183**, 519-528
64. Legrain, C., Halleux, P., Stalon, V., and Glansdorff, N. (1972) *Eur J Biochem* **27**, 93-102
65. Weber, K. (1968) *J Biol Chem* **243**, 543-546
66. Cunin, R., Wales, M. E., Van Vliet, F., De Staercke, C., Scapozza, L., Rani, C. S., and Wild, J. R. (1996) *J Mol Biol* **262**, 258-269
67. England, P., and Hervé, G. (1992) *Biochemistry* **31**, 9725-9732

Legends to figures

FIG 1. The arginine biosynthetic pathway and its regulations

FIG 2. Simplified representation of the arginine biosynthetic pathway and its regulations. 1-3: modules; RB: rigid branch point

FIG. 3 Cross-feeding experiments demonstrate metabolite secretion. Potential secretors are streaked on the left side and indicators on the right. (**A**) P4XB2 (*argR*) and (**B**) P4XA1 (*argA-216*) strains secrete arginine and allow growth of indicator PA342; (**C**) the double mutant P4XA1-ΔR secretes high amounts of arginine and indicator PA342 was fully grown after 16 hours incubation, while 50 hours were necessary to see equivalent growth on plates (**A**) and (**B**). A strain with constitutive low CPSase synthesis accumulates and secretes ornithine and allows growth of the indicator P4XEC-1 (**D**), but not of PA342 (**E**).

FIG. 4 Simulated variation of arginine (**diamonds**), ornithine (**squares**) and CP (**triangles**) concentrations in function of CPSase cellular maximal velocity (V_{MC}). Small symbols represent simulation results, while larger symbols correspond to experimental results for the wild-type *E. coli* on minimal medium. Simulation results were obtained by integration of the model defined by eqs (1)-(10), with the parameter values indicated in Table III, except for V_{MC}, which is as indicated.

FIG. 5 Relative free arginine concentrations (wild-type = 1.0) in different simulated conditions (black bars). Simulation results were obtained by integration of the model defined by eqs **(1)-(10)**, with the parameter values indicated for the wild-type in Table III and by introducing specific perturbations. (A) wild-type; (B) wild-type with an increased CPSase capacity (CPSase = 2.5 mM min^{-1}); (C) wild-type with a doubled glutamate concentration (14 mM); condition; (D) combination of (B) and (C); (E) genetic derepression; (F) feedback-resistant NAGSase; (G) combination of (F) and (C); (H) combination of (E) and (F). When available, experimental results (grey bars) are shown alongside the model predictions.
Inset: to avoid compression due to the size of bar H, bars A to G are shown with an expanded scale for arginine concentrations.

Gene name	Enzyme name	EC nr
argA	N-acetylglutamate synthase	2.3.1.1
argB	N-acetylglutamate kinase	2.7.2.8
argC	N-acetylglutamylphosphate reductase	1.2.1.38
argD	Acetylornithine transaminase	2.6.1.11
argE	N-acetylornithinase	3.5.1.16
argF	Ornithine transcarbamylase	2.1.3.3
argI	Ornithine transcarbamylase	2.1.3.3
argG	Arginosuccinate synthase	6.3.4.5
argH	Argininosuccinate lyase	4.3.2.1
carA	Carbamyl phosphate synthase, subunit A	6.3.5.5
carB	Carbamyl phosphate synthase, subunit B	6.3.5.5

Table I Genes and enzymes of arginine biosynthesis

Table II Values of the parameters that do not change with strains or experimental conditions. These values were used in all the simulations.

Parameters	Description	Value	Source
General			
Volume of *E.coli*		10^{-15} l	www.projectcybercell.com
Protein per cell		3.61 10^{-13} g	This study
K_U	K for arginine utilization	0.15 mM	*Estimated
V_{MU}	Rate of arginine utilization	0.18 mM min^{-1}	*Estimated
$P_a \theta_{ext}$	Rate of arginine uptake	0.14 mM min^{-1}	*Estimated
K_F	K for ornithine secretion and consumption for polyamine synthesis	0.5 mM	*Estimated
K_{pyr}	K for nucleotides supply by the salvage pathway	0.05 mM	*Estimated
NAGSase			
V_{max}	Maximal velocity	432 U mg^{-1}	(32)
MW	Molecular weight	300.000	(60)
K_1	K_m for glutamate	25 mM	(32)
K_2	K_m for acetyl CoA	5 mM	(32)
S_2	Acetyl CoA concentration	5 mM	*Estimated
ρ	Arginine inhibition scaling factor	0.25	Deduced from the rate equation
$K_{i\theta}$	K inhibition by arginine for the wild-type enzyme	0.11 mM	(32)
$K_{i\theta}$	K inhibition by arginine for a feed-back resistant enzyme	3.8 mM	(32)
CPSase			
S_3	Bicarbonate concentration	10 mM	*Estimated
V_{max}	Maximal velocity	150 U mg^{-1}	(61)
MW	Molecular weight	160.000	(62)
K_3	K_m for bicarbonate	3.6 mM	(63)
K_4	K_m ATP of CPSase, if IMP is present	3.8 mM	Calculated, based on (21)
K_4	K_m ATP of CPSase, if IMP is low or absent	10.4 mM	Calculated, based on (21)
K_5	K_m for glutamine	0.22 mM	(63)
$K_{I\gamma}$	K of inhibition by UMP	0.02 mM (0.05-0.005)	(63)
$K_{A\beta}$	K of activation by ornithine	0.1 mM	(63)
η	Variation of K_m due to the presence of UMP	10	Fit to ATP saturation curve (63)
ζ	Variation of K_m due to the presence of ornithine	0.1	Fit to ATP saturation curve (63)
OTCase			
V_{max}	Maximal velocity	120000 U mg^{-1}	(64)
MW	Molecular weight	105.000	(64)
$K_{\alpha 1}$	K_m for CP	0.12 mM	(63)
K_β	K_m for ornithine	1.38 mM	(63)
ATCase			
V_{max}	Maximal velocity	24000 U mg^{-1}	(30)
MW	Molecular weight	306.000	(65)
$K_{\alpha 2}$	K_m for CP	0.9 mM	(63)
K_6	Average K_m for aspartate**	7 mM	(66)
$K_{i\delta}$	K inhibition by CTP and UTP	0.5 mM (0.009-0.81)	(67)
n_6	Hill coefficient	2	Fit to aspartate saturation curve (36)

*Estimated: obtained by manual adjustment to obtain the appropriate steady-state for the wild-type on minimal medium.

**In the presence of the activator ATP (66)

Table III System calibration. To calibrate the model, we used data from the wild-type, both in minimal medium and in arginine-rich medium. Parameters indicated as "measured" were determined experimentally and then used in the simulations. Parameters indicated as "estimated" were fitted so as to obtain by simulation with the model the same steady-state values for the metabolite concentrations as those measured experimentally. (A) Values of the parameters that were used for the calibration of the model; experimental measurements show those that were different in minimal or in arginine-rich medium; (B) Measured and simulated values of the steady-state concentrations of the metabolites (variables of the system).

A

Parameters	Description	Values		Source
S_1	Glutamate concentration	7.00 mM		Measured
S_4	ATP concentration	2.50 mM		Measured
S_5	Glutamine concentration	0.50 mM		Measured
S_6	Aspartate concentration	0.30 mM		Measured
[IMP]	IMP concentration	0.50 mM		Measured
K_4	K_m ATP of CPSase	3.80 mM		(20)
J_o	Rate of UMP generation by the pyrimidine salvage and inter-conversion pathways	0.09 mM min^{-1}		Estimated
k_2	Rate constant for UTP and CTP synthesis from UMP	0.085 min^{-1}		Estimated
k_3	Rate constant for UTP and CTP utilization by the cell	0.07 min^{-1}		Estimated
		Minimal medium	**Arginine-rich medium**	
V_{MN}	Cellular maximal velocity of NAGSase	2.65 mM min^{-1}	1.10 mM min^{-1}	Measured
V_{MC}	Cellular maximal velocity of CPSase	2.10 mM min^{-1}	0.80 mM min^{-1}	Measured
V_{MO}	Cellular maximal velocity of OTCase	417.00 mM min^{-1}	10.00 mM min^{-1}	Measured
V_{MA}	Cellular maximal velocity of ATCase	76.00 mM min^{-1}	61.00 mM min^{-1}	Measured
V_{MF}	Rate of ornithine secretion or utilization for polyamine synthesis	0.25 mM min^{-1}	0.25 mM min^{-1}	Estimated
k_s	Rate constant for arginine secretion	0.00 min^{-1}	0.00 min^{-1}	Estimated

B

	Minimal medium		**Arginine-rich medium**	
	Measured	Simulated	Measured	Simulated
CP (α)		$4\ 10^{-3}$		3.21
ornithine (β)	≤0.02	$8\ 10^{-3}$	≤0.02	$3\ 10^{-3}$
arginine (θ)	0.14 ± 0.03	0.14	1.5 ± 0.3	1.51
UMP (γ)	1.1 ± 0.2	1.01	1.0 ± 0.2	1.10
CTP+UTP (δ)	1.5 ± 0.3	1.23	1.4 ± 0.2	1.32
UMP (γ)*	1.1 ± 0.3	1.03	1.3 ± 0.2	1.17
CTP+UTP (δ)*	1.6 ± 0.3	1.26	1.6 ± 0.3	1.42

Intracellular concentrations in mmoles l^{-1}

* UMP and CTP+UTP intracellular concentrations when cells are grown in media containing 5 mM aspartate

Table IV Model validation. Values of the parameters used in the simulations whose results are given in Table V. These values were determined experimentally, except for K_4 (which is modified according to (20) because of the change in [IMP]), k_S (which reflects arginine secretion, a process which is known to be up-regulated by arginine) and the parameters characterizing pyrimidine synthesis (which are fitted to get the appropriate levels of pyrimidines).

Parameters	Genetic derepression (*argR* mutated, P4XB2)		No feedback inhibition (fbr-NAGSase mutant, P4XA-1)		Limited CP synthesis (constitutive low CPSase, P4XJEF8/pMAC2)		Source
S_1	5.50 mM		11.00 mM		10.00 mM		Measured
S_4	2.50 mM		2.50 mM		2.50 mM		Measured
S_5	1.20 mM		0.50 mM		0.90 mM		Measured
S_6	0.36 mM		0.30 mM		0.20 mM		Measured
[IMP]	0.90 mM		0.50 mM		0.10 mM		Measured
K_4	3.80 mM		3.80 mM		10.40 mM		(20)
J_o	0.180 mM min^{-1}		0.090 mM min^{-1}		0.065 mM min^{-1}		Estimated
k_2	0.085 min^{-1}		0.085 min^{-1}		0.085 min^{-1}		Estimated
k_3	0.070 min^{-1}		0.070 min^{-1}		0.040 min^{-1}		Estimated
	Minimal medium	**Arginine-rich medium**	**Minimal medium**	**Arginine-rich medium**	**Minimal medium**	**Arginine-rich medium**	
V_{MN}	8.00 mM min^{-1}	6.40 mM min^{-1}	2.10 mM min^{-1}	0.61 mM min^{-1}	2.85 mM min^{-1}	1.60 mM min^{-1}	Measured
V_{MC}	3.40 mM min^{-1}	2.60 mM min^{-1}	2.40 mM min^{-1}	1.00 mM min^{-1}	0.40 mM min^{-1}	0.63 mM min^{-1}	Measured
V_{MO}	4516.00 mM min^{-1}	4516.00 mM min^{-1}	494.00 mM min^{-1}	20.00 mM min^{-1}	4736.00 mM min^{-1}	33.00 mM min^{-1}	Measured
k_s	0.002 min^{-1}	0.025 min^{-1}	0.002 min^{-1}	0.01 min^{-1}	0.00 min^{-1}	0.00 min^{-1}	Estimated

Table V. Model validation. Simulated and measured intracellular metabolite concentrations in perturbed conditions. Simulations used parameter values from Tables II and IV.

	Genetic derepression (*argR* mutant, P4XB2)			
	Minimal medium		**Arginine-rich medium**	
	Simulated	Measured	Simulated	Measured
CP (α)	$5\ 10^{-4}$		$5\ 10^{-4}$	
ornithine (β)	0.01	≤0.02	$8\ 10^{-3}$	≤0.02
arginine (θ)	0.82	0.83 ± 0.08	3.30	3.4 ± 0.3
UMP (γ)	2.07	2.1 ± 0.3	2.07	2.2 ± 0.2
CTP+UTP (δ)	2.51	2.3 ± 0.2	2.51	2.5 ± 0.2
	No feedback-inhibition (fbr-NAGSase mutant, P4XA-1)			
	Minimal medium		**Arginine-rich medium**	
	Simulated	Measured	Simulated	Measured
CP (α)	$1\ 10^{-3}$		0.08	
ornithine (β)	0.06	0.05 ± 0.1	$7\ 10^{-3}$	≤0.02
arginine (θ)	0.91	1.0 ± 0.1	1.56	1.6 ± 0.3
UMP (γ)	1.01	1.10 ± 0.07	1.01	1.2 ± 0.2
CTP+UTP (δ)	1.23	1.3 ± 0.1	1.23	1.3 ± 0.2
	Limited CP synthesis (constitutive low CPSase, P4XJEF8/pMAC2)			
	Minimal medium		**Arginine-rich medium**	
	Simulated	Measured	Simulated	Measured
CP (α)	$5.5\ 10^{-6}$		$2\ 10^{-3}$	
ornithine (β)	0.43	0.41 ± 0.04	0.06	≤0.02
arginine (θ)	0.06	0.05 ± 0.005	1.42	1.4 ± 0.1
UMP (γ)	0.71	0.70 ± 0.06	0.72	0.8 ± 0.05
CTP+UTP (δ)	1.52	1.5 ± 0.1	1.53	1.6 ± 0.1

Concentrations in mmoles l^{-1}

FIG .1

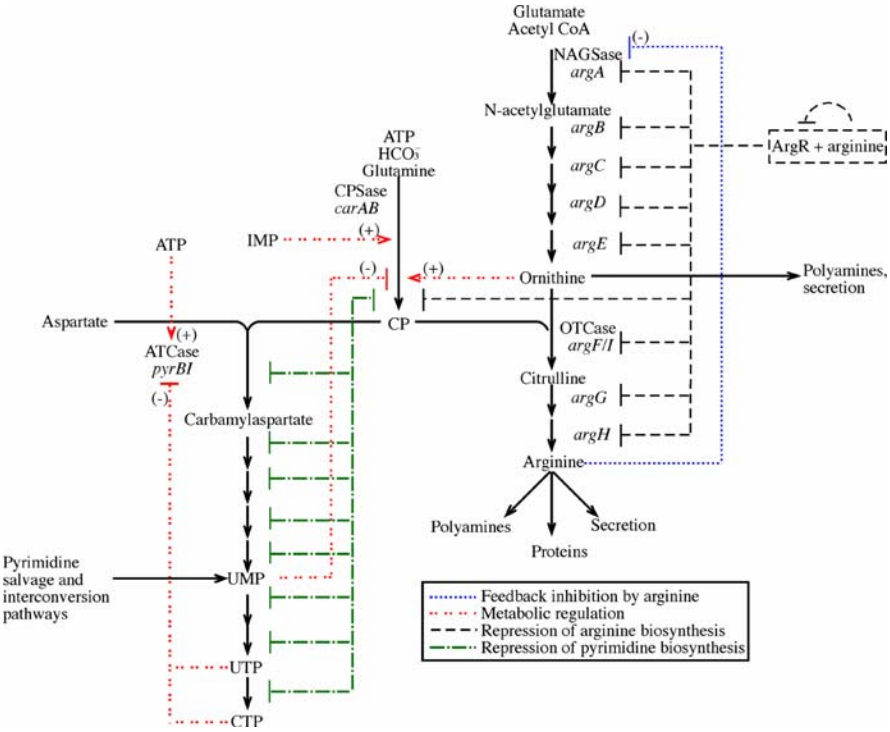

FIG. 2

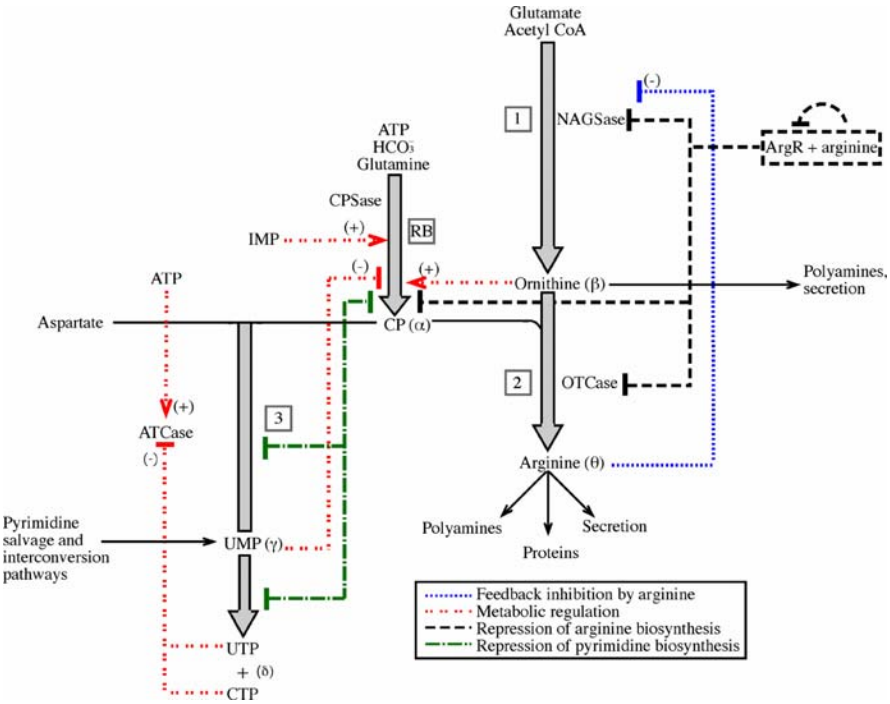

FIG. 3

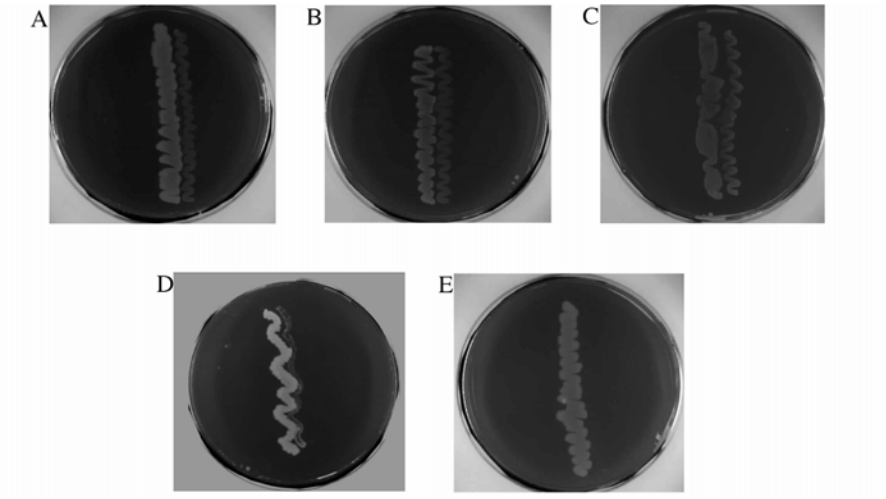

FIG. 4

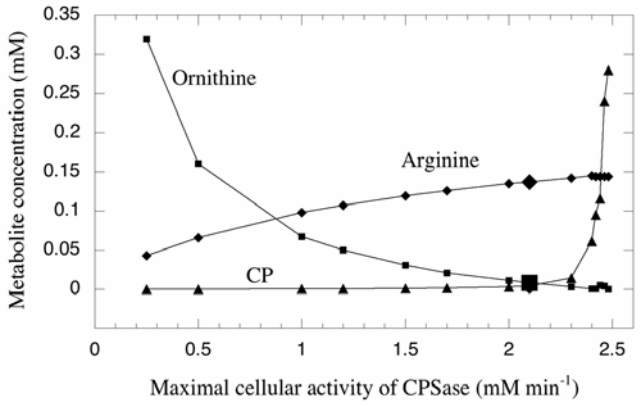

FIG. 5